Acta Medica et Biologica
Vol. 38, (Suppl.), 55-67, 1990

Pathological Analysis of Sclerotic Changes of the Glomerulus

Kazunari IIDAKA, Yoshihiko UEDA, Kaoru HIRABAYASHI and Hidehiko ONO

Department of Pathology, Dokkyo University School of Medicine, Tochigi, Japan

Received October 20, 1989

Summary. **Clinico-pathological analysis of focal glomerular sclerosis (FGS) on repeated renal biopsies were made. It was revealed that sizes of capillary lumina in prospective findings of FGS were considered to be larger than those in lipoid nephrosis. ($P<0.01$)**

In order to show morphological characteristics of glomeruli in the juxtamedullary cortex of the human kidney, the number of glomeruli and glomerular size in subcapsular and juxtamedullary cortex were compared. Average values obtained by morphometric study per 1 mm^2 were 3.2 glomeruli in the subcapsular and 2.0 glomeruli in the juxtamedullary cortex. Juxtamedullary glomeruli were larger than those in the subcapsular ($P<0.05$).

The luminal diameter of afferent and efferent arteiole in different cortical regions were measured morphologically by scanning electron microscopy using methyl metacrylate casts of renal arterial trees.

Afferent arterioles in the subcapsular glomeruli were larger than efferent arterioles. However, efferent arterioles in the juxtamedullary glomeruli were statistically equal to or larger than afferent arterioles.

In order to examine anionic sites in the mesangium by intravenous administration of polyethyleneimine (PEI) as a cationic probe, an experimental AN nephrosis model was designed. PEI particles were most numerous in the subendothelial regions in the control. In the group treated with aminonucleoside of puromycin, numbers of PEI particles significantly decreased in each mesangial region, particularly in the paramesangial region.

Arterial cushions in the rat kidney were cleary discernible in the arcuate and interlobular arteries but not those in the subcapsular areas. They were stained positively and clearly with colloidal iron.

Anionic loss in the mesangial matrix and arterial cushions may be an important etiological factor of glomerulosclerosis.

INTRODUCTION

Histological diagnosis of focal segmental glomerular sclerosis (FGS) is one of the most difficult renal biopsy procedures. Success depends on whether the glomerular lesions, seen by light microscopy, are focal-segmental in distribution. Glomerular lesions of FGS are most prominent and appear first in the juxtamedullary cortex (vulnerability of glomerular lesion) and extend from the corticomedullary junction to progressively involve superficial cortical glomeruli. Other glomeruli are normal or show minor abnormalities on light microscopy.

Clinically, FGS is a progressive non-proliferative renal disease associated with persistent microscopic hematuria, steroid-resistant proteinuria and frequently with nephrotic syndrome. Although FGS was initially thought to represent an end stage of lipoid nephrosis,[1,2] recent opinions suggest the two diseases are separate and independent entities.[3] We therefore differentiate FGS from lipoid nephrosis.

1. Morphological definition of the FGS lesion

Microscopic findings can be characterized by the following three categories. 1) Many of the glomeruli show minor abnormalities on light microscopy. Others exhibit solidification of one or more lobules of the capillary tufts with sclerosis, and the affected lobule is adherent to the Bowman's capsule. Foam cells and hyalinosis within sclerotic lesions are important findings. It is reported that foam cells were found in 78 percent of cases.[4] When hyaline deposition is not observed, the alternative diagnosis of resolved focal glomerulonephritis cannot be excluded. 2) Glomeruli

affected with segmental sclerosis occur predominantly in the juxtamedullary zone.[2] If the renal biopsy specimen does not include the juxtamedullary region, typical focal-segmental glomerular lesions may not be present and the mistaken diagnosis of lipoid nephrosis may be made. 3) Regarding immunofluorescence microscopy findings; in segmental sclerotic areas, IgM usually in combination with C3 is commonly found. IgG and IgA have also been recorded in these areas but their staining is not observed as constantly or intensely as IgM.

In the unaffected glomeruli or unaffected part of tuft in the glomeruli with segmental sclerotic lesions, neither immunoglobulin nor its complement is generally found.

These immunoglobulins are supposed to be unrelated to immunological activity. They are considered accumulations or entrapments of IgM within the sclerotic lesion.

2. Clinico-pathological analysis of FGS on renal biopsies

64 cases of FGS were examined histologically (data were provided by Progressive Glomerular Injury Research Committee, The Ministry of Health and Welfare, Japan. Group leader: Dr. Tojo, S., 1988). These included 26 cases who received more than one biopsy, 24 cases underwent 2 biopsies and 2 cases underwent 3 or 4. In these cases, the relation between prognosis and a proportion of glomerular lesion (GSR; sclerotic glomeruli/total numbers of glomeruli $\times 100$) was examined. The cases were classified into four groups based on laboratory data, mainly with reference to proteinuria, BUN, Cr., and Ccr. at the initial biopsy and prognosis after the follow-up period.

Group 1; clinical data were favorable at the biopsy and remained on a favorable clinical course.

Group 2; unfavorable shift to favorable.

Group 3; favorable shift to unfavorable.

Group 4; unfavorable to unfavorable.

The difference between group 1 and group 4 is seen as statistically significant ($p<0.01$) in Table 1. Characteristic or qualitative glomerular changes and prognosis were not found but severe tubulointerstitial changes corresponded to the poor prognosis group.

3. Possible earlier glomerular changes in FGS

On light microscopy, it is possible that early changes of FGS may be detected as minor glomerular abnormalities based on serial biopsies of FGS. The subjects were initial biopsy specimens which later progressed to FGS on the 2nd or 3rd biopsy. Findings are categorized as follows. 1. Vacuolic changes of glomerular epithelial cells. 2. Irregularities and dialation of the tuft capillary lumen. 3. Localized proliferation of parietal epithelial cell and partial thickening of Bowman's basement membrane. 4. IgM deposition in mesangial areas in glomeruli with minor change.

Table 1. Correlation between prognosis and percentage of glomerular sclerosis of renal biopsies on patients with FGS.

	Group 1	Group 2	Group 3	Group 4
no. of cases	16	18	11	19
% of GS	32.1±17.4	37.9±29.2	45.3±25.3	57.1±25.5

W-test ** : $p<0.01$ * : $p<0.05$

Group 1; clinical data were favorable and remained in favorable clinical course after follow-up period. (Judging from these by laboratory data)
Group 2; unfavorable to favorable.
Group 3; favorable to unfavorable.
Group 4; unfavorable to unfavorable.
GS; glomerular sclerosis.

Irregularity of lumen and dilatation of capillaries are particularly significant in the above-mentioned findings. Therefore, concerning item 2, morphometrical measurements of glomerular capillary areas by the computer-imaging analytical method were made with light micrographs regarding the following three groups of glomerular lesions.

Group 1: Minor glomerular abnormalities which progressed to FGS on serial biopsy in four cases.

Group 2: Non-sclerotic glomeruli in six cases of FGS.

Group 3: Minor changes of glomeruli in lipoid nephrosis in six cases.

Results showed areas of capillary lumen and standard deviation in group 1 were larger than group 3 (Table 2).

Therefore, it is suggested that progress of minor glomerular change to segmental screrosis depends upon the irregular size of capillary lumen of glomerular tufts. Sizes of capillary lumina in prospective FGS were considered to be larger than those in lipoid

Table 2. Comparison of areas of glomerular capillary lumina in minor glomerular changes.

	Group 1	Group 2	Group 3
no. of capillaries	855	841	1095
mean (μm^2)	90.9	69.1	43.0
	*	*	
	*		
S.D.	88.6	60.5	30.9
	**	**	
	**		

* : $p<0.01$ (T-test) ** : $p<0.01$ (F-test)

Group 1; minor glomerular abnormalities which progress to FGS on serial biopsy.
Group 2; non-sclerotic glomeruli in patient with FGS.
Group 3; minor change glomeruli in lipoid nephrosis.

nephrotic syndrome.

4. Morphometrical analysis of the glomerulus and arterioles

Numbers and size of glomeruli in the different cortical layers

Numbers of glomeruli per unit area of 1 mm^2 in each layer (subcapsular, mid-cortex and juxtamedullary cortex) were determined by ordinary light microscopic slides of material obtained from four autopsy kidneys.

Table 3. Number of glomeruli in different layers of cortex per 1 mm^2.

	SC	MC	JM	mean
case A	3.5±1.52	2.8±1.55	2.4±1.21	2.9
case B	3.1±1.34	2.9±1.60	2.5±1.03	2.8
case C	3.2±1.67	2.6±1.34	1.6±0.92	2.5
case D	3.1±1.87	1.9±1.31	1.5±1.20	2.2
mean	3.2	2.6	2.0	

(M±SD)

SC; subcapsular cortex. MC; mid-layer of cortex. JM; juxtamedullary cortex.

Average values obtained by morphometric study of glomeruli per 1 mm^2 in the four cases are as follows; 3.2 glomeruli in the subcapsular cortex, 2.6 glomeruli in the cortex mid-portion and 2.0 glomeruli in the juxtamedullary cortex (Table 3). Statistical significance between the subcapsular and juxtamedullary cortex was evaluated, with fewer glomeruli in the juxtamedullary cortex than the corresponding value in subcapsular area (W-test).

To accurately determine glomerular size, measur-

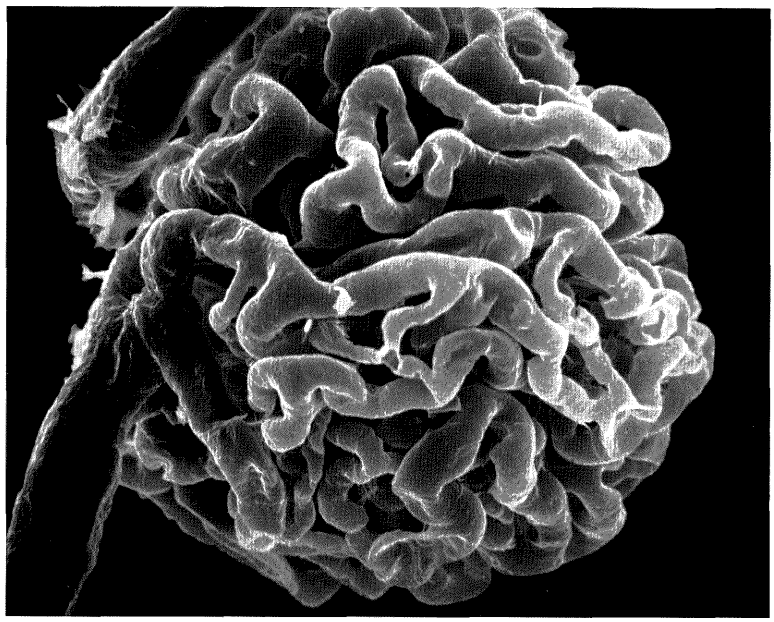

Fig. 1. SEM of methyl metacrylate cast of glomerular tufts.

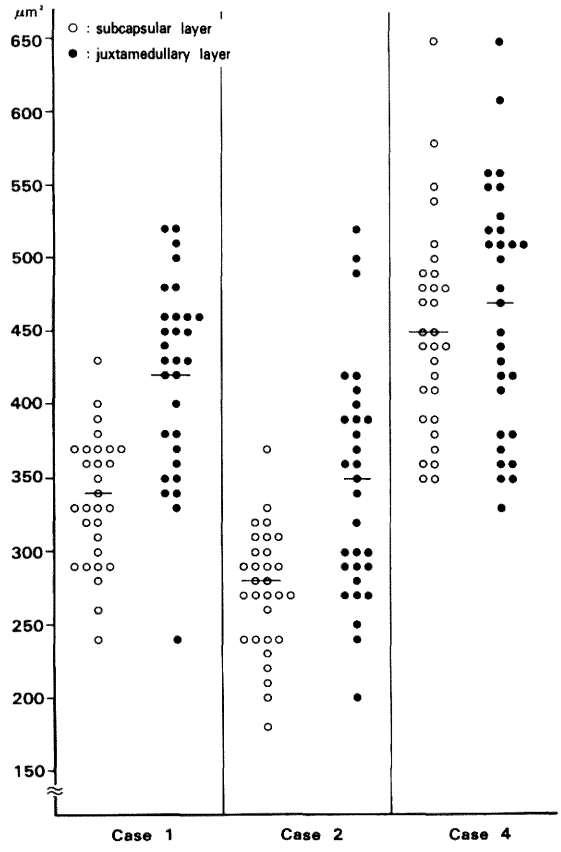

Fig. 2. Morphometrical analysis of glomerular size in different cortical layers.

ment was made with scanning electron micrographs of methylmetacrylate casts of glomeruli (Fig. 1) from different layers of the cortex. Materials were obtained from three autopsied kidneys without renal diseases.

Average values of maximum measurement of glomerular vascular casts by scanning electron micrographs were examined. Average values obtained are shown in Fig. 2. Case No. 3 was not available for examination. Values of glomerular size were larger in the juxtamedullary cortex in both cases and significant statistical differences were noted ($p<0.05$) (Fig. 2).

Morphometrical analysis of afferent and efferent arterioles in the different cortical layers

To elucidate differences in intrarenal hemodynamics and glomerular function between the subcapsular and juxtamedullary cortices, we investigated aspects of intrarenal arterial structure and sizes of small artery and arteriole internal diameters, including glomeruli, by scanning electron micrography of plastic models (Fig. 3).[5] The materials mentioned above were used. Afferent arterioles, after reaching the vascular pole of the glomerulus, branched to three or four main capillaries in more than 60 percent of glomeruli.

Oval-shaped impressions (possibly representing the endothelial nuclei) in afferent arterioles and longitudinal folds in efferent arterioles were noted (Fig. 4).

The difference in the main capillary branch num-

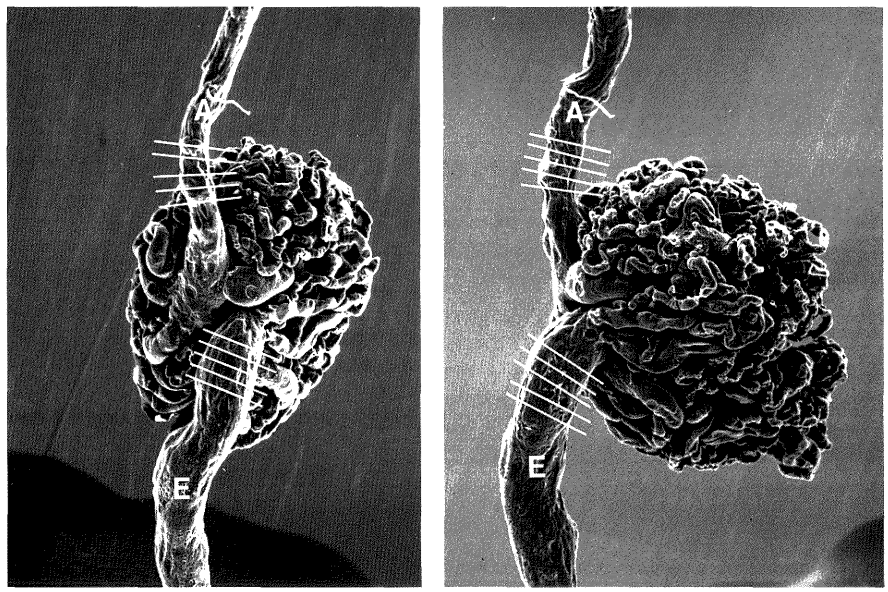

Fig. 3. SEM of methyl metacrylate cast of arterioles to show quantitative estimates of internal diameter. A; afferent artery. E; efferent artery.

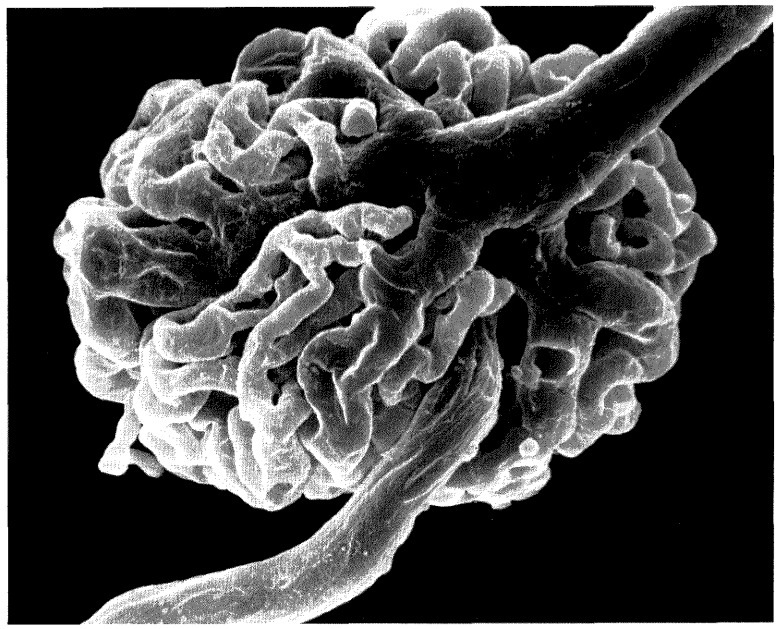

Fig. 4. SEM of methyl metacrylate cast of afferent and efferent arteries.

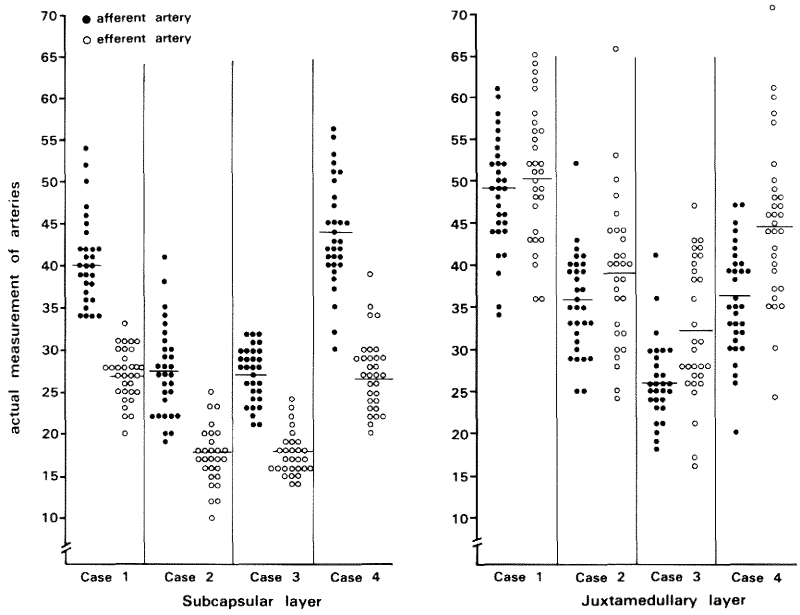

Fig. 5. Morphometrical analysis of afferent and efferent arteries in different layers of cortex.

bers from the afferent artery between layers (subcapsular and juxtamedullary) was not significant. However, afferent and efferent arteriole internal diameters showed differences in both layers. Afferent arterioles in the subcapsular glomeruli were larger than efferent arterioles.

The internal diameters of efferent arterioles in the juxtamedullary glomeruli were statistically equal or larger than those of afferent arterioles (t-test) (Fig. 5). Furthermore, standard deviation of numerical values

of efferent arterioles in the juxtamedullary glomeruli showed great variation.

5. Glomerular sclerosis from a viewpoint of experimental models using aminoncleoside nephrosis

Materials and methods

Male Sprague-Dawley rats aged 1 month (body weight approximately 100 g) were divided into two groups, AN-I, II, III, (Aminonucleoside of puromycin (PA)-treated groups) and C-I, II, III, (saline-treated groups as control). The AN-I group received 10 mg/100 g BW of PA in a single intraperitoneal dose, and was sacrificed after 30 days. Another subgroup, designated as AN-II, received a second equal dose of PA 30 days after the first, and was sacrificed on the 60th day, while subgroup AN-III received additional doses of PA on both the 30th and 60th days after the first and was sacrificed on the 90th day. Rats in the control group received physiological saline in place of PA, and the corresponding subgroups were designated as C-I, C-II and C-III. Colloidal iron and PEI were used as cationic probes.

Observation using PEI was conducted in accordance with method of Schurer et al.[6] That is, 0.2 ml/100 g BW of 0.5% PEI (MW 40,000-60,000, PH 7.4, 400 mOsm; Sigma) was administered via the caudal vein 15 min prior to sacrifice. The peripheral portion of GBM per 0.33 μm length and the areas of mesangial matrix three nonsclerotic glomeruli were examined in each animal. The numbers of PEI particles in these areas were measured with a graphic analysis system, the number of particles per 0.1 μm^2 was calculated in each cases, and statistical analysis was performed by applying the t-test to mean values. Sites measured in the mesangium were divided into three regions: the central region of the mesangial matrix (CM), the paramesangial region of the mesangial matrix (PM) and the subendothelial region of the mesangial matrix (SEM).

The data were analysed with reference to each of these three regions.

Results of the experimental model of AN nephrosis

Anionic sites in GBM:

Electron microscopically, severe vacuolic change in glomerular epithelial cells was initially noted with subsequent loss of polyanion with fusion of foot processes in the non-sclerotic tufts. The loss of negative charge in some areas occured before epithelial foot process fusion. The mean number of PEI particles decreased significantly in AN groups predominantly in the lamina rara externa in the early group (AN-I), and at the later stage (AN-III), and decreased also in the lamina rara interna in the later stage (AN-III) (Table 4).

Table 4. Number of PEI particles in GBM per unit length of 0.33 μm.

		I	II	III
LRE	C	6.3±1.6	4.6±1.1	4.7±0.8
	AN	5.2±1.2	4.2±1.3	3.9±1.2
		**		**
LRI	C	4.6±1.8	4.1±1.5	3.5±1.4
	AN	3.9±1.5	3.2±1.6	2.5±0.9
			*	**

** : $p<0.01$ * : $p<0.05$

LRE; lamina rara externa. LRI; lamina rara interna.
AN; aminonucleoside nephropathy. C; control.
I; sacrificed on 30th day. II; 60th day. III; 90th day.

Table 5. Number of PEI particles in mesangial matrix per 0.1 μm^2.

	I	II	III
C	12.9±3.7	12.5±4.2	13.1±4.2
	*	*	*
AN	10.2±4.3	10.6±4.4	9.4±4.0

T-test, * : $p<0.01$ (mean±S.D.)

AN; aminonucleoside nephropathy. C; control.
I, II, and III; the same as Table 4.

Anionic sites in the mesangial matrix:

This study aimed to elucidate pathogenesis of the sclerotic lesions in AN nephrosis, and investigated various aspects of the anionic sites in different regions of the mesangial matrix.

Analysis of the mean numbers of PEI particles per 0.1 μm^2 in the mesangial matrix revealed a significant decrease in AN groups (I, II, III) compared with the control group in all three mesangial regions, as well as in the GBM (Table 5, Figs. 6, 7).

In the control group, the mean number of PEI particles in the SEM region was the highest among the three different regions of mesangial matrix. In

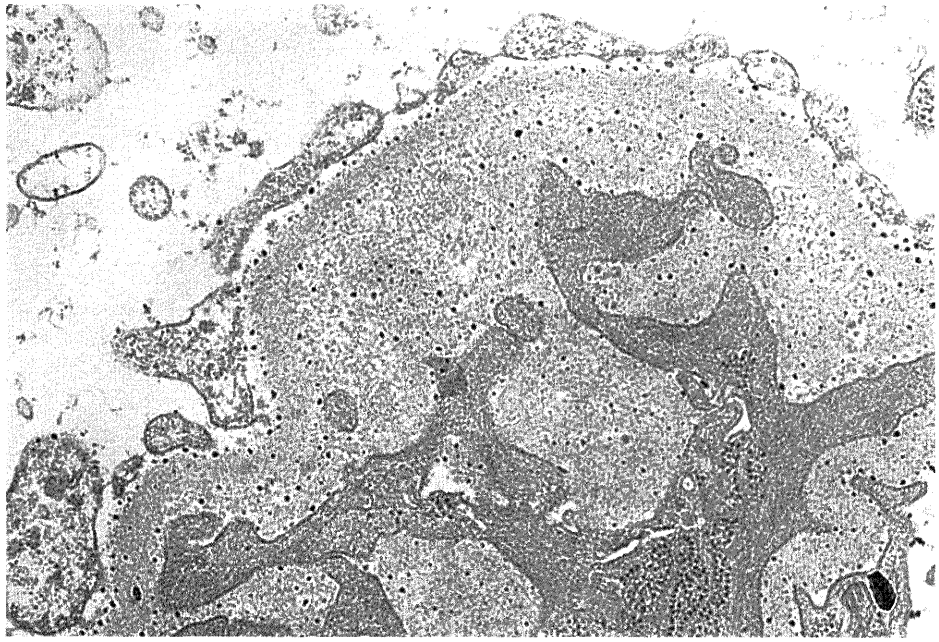

Fig. 6. Electron micrograph showing PEI particles in the paramesangial region of mesangial matrix in control group. ×2,400

Fig. 7. Electron micrograph showing PEI particle in the paramesangial region of mesangial matrix in AN-III group. ×3,000

the AN groups the numbers of particle were also high in the SEM region. The CM and PM regions were next in order of PEI particle counts, with the PM region being the lowest (Table 6).

Additionally, in order to investigate the relation between findings in the AN groups and charge depletion in the three mesangial regions, mean values in the control group were regarded as 100%, and temporal changes in the mean values for each of the three mesangial regions were plotted (Fig. 8). In the CM region, the charge progressively decreased with passage of time while in the PM region, the values

Table 6. Number of PEI particles in three different regions of mesangial matrix.

CM

	I	II	III
C	12.47±4.40	12.44±4.58	13.72±4.43
AN	11.17±6.51	10.32±4.36	9.77±4.25
		*	**

PM

	I	II	III
C	12.12±3.47	11.26±3.60	11.53±2.96
AN	8.65±2.22	8.05±2.83	7.50±2.79
	**	**	**

SEM

	I	II	III
C	14.19±2.07	13.87±4.02	13.84±4.51
AN	10.98±3.21	12.45±4.78	10.17±3.50
	**		**

T-test, ** : $p<0.01$ * : $p<0.05$ (mean±S.D.)

CM; central region. PM; paramesangial region. SEM; subendothelial region. AN; aminonucleoside nephropathy. C; control. I, II, and III; the same as Table 4.

were roughly 65-70%, which was lower than the corresponding values in the other two regions for each of the AN-I, AN-II and AN-III subgroups.

Center-to-center distances between the PEI particles in all three mesangial regions ranged from about 40 nm to more than 100 nm, with a large standard deviation, and the regular distribution seen in the GBM was not observed in the mesangial matrix.

Morphological features of the "arterial cushion" in the kidney

The distribution and morphology of arterial cushions were studied in rat renal arteries by light microscopy, transmission electron microscopy and scanning-electron microscopy using renal vascular

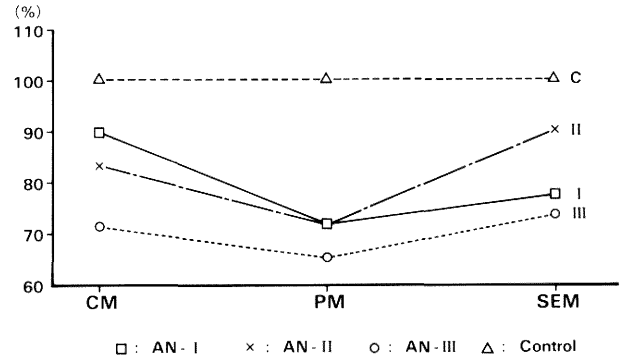

Fig. 8. Comparison of PEI particles in different regions of mesangial matrix. CM; central region of mesangial matrix. PM; paramesangial region of mesangial matrix. SEM; subendothelial region of mesangial matrix. AN-I, AN-II and AN-III; the same as Table 4.

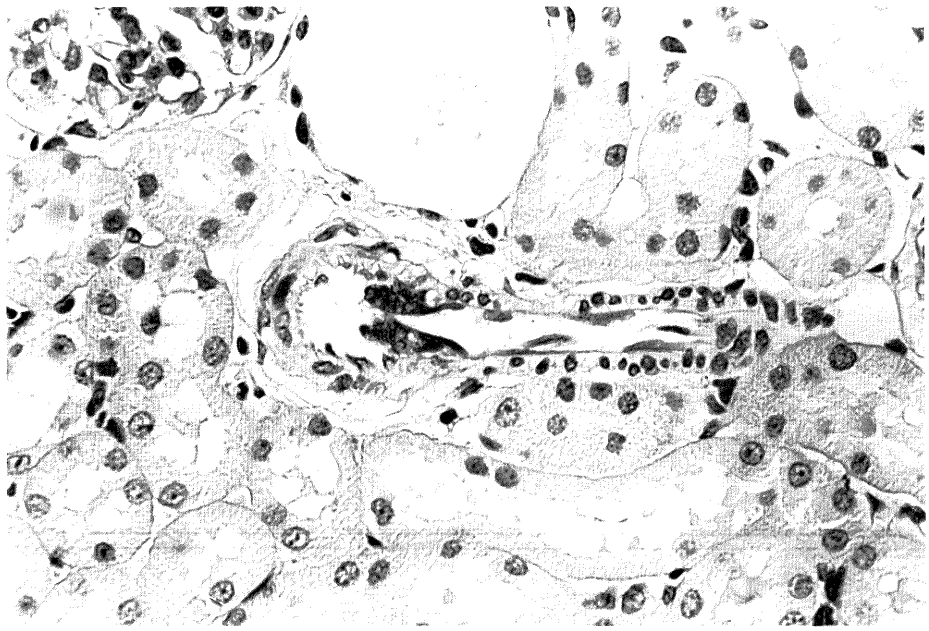

Fig. 9. Arterial cushion at a region of branching artery from interlobular artery in rat. Colloidal iron stain. ×300

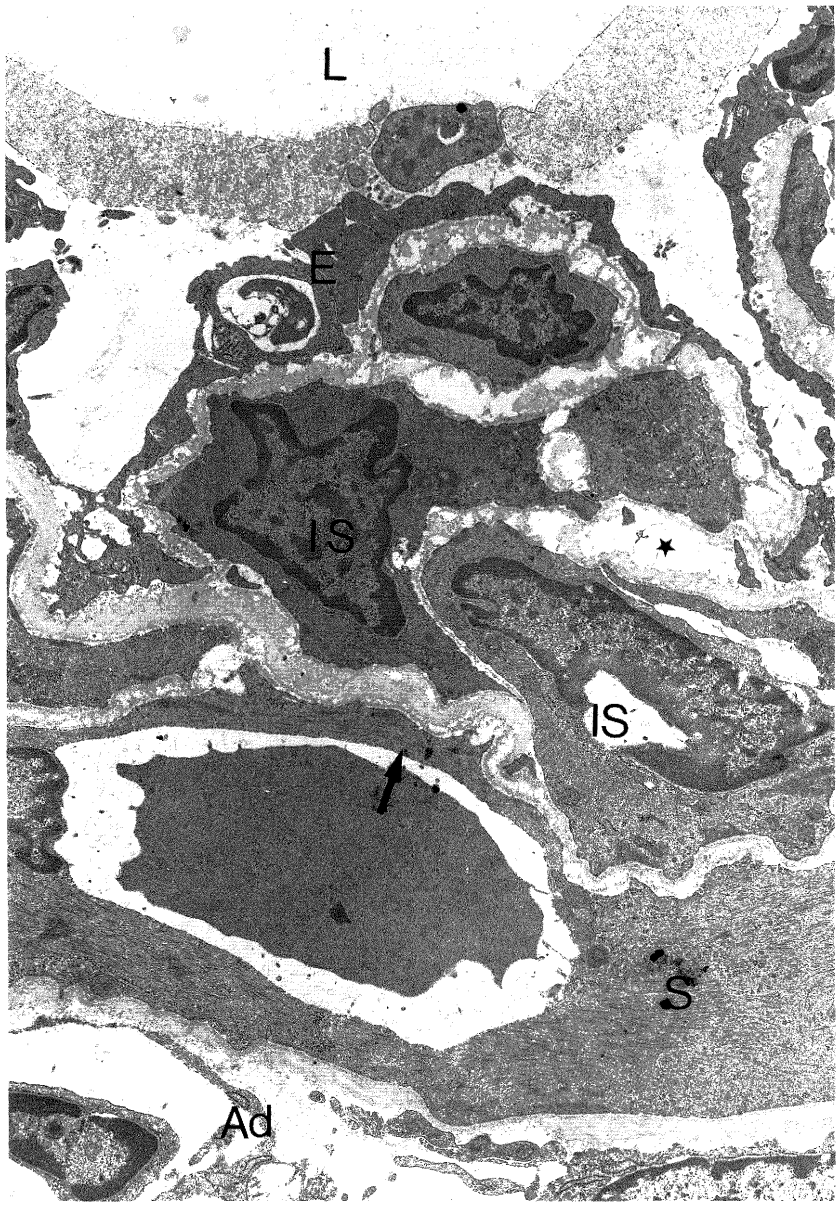

Fig. 10. Electron micrograph showing arterial cushion in bifurcation of interlobular to afferent artery. Modified smooth muscle cells (*IS*) are surrounded by interstitial matrix (★). Surface of cushion is covered by thin endothelial cells (*E*). S: medial smooth muscle cells. Ad: adventitia. ↑ : internal elastic membrane. ×7,200

casts similar to those mentioned above.

The arterial cushions were observed at the region of the branching arteries from the arcuate and the interlobular arteries (Fig. 9). They were found frequently by serial section light microscopy in the mid-cortex and juxtamedullary cortex, but not in the subcapsular cortex. The arterial cushion and GBM were both positively and clearly stained with colloidal iron staining (Fig. 9).

Under transmission electron microscopy, the arterial cushion showed valve-like protrusions into the vascular lumen and consisted of three components, endothelial cells, smooth muscle cells and interstitial ground substances (Fig. 10). The cushions were covered by endothelial cells which often showed variations in thickness. These had deep processes which

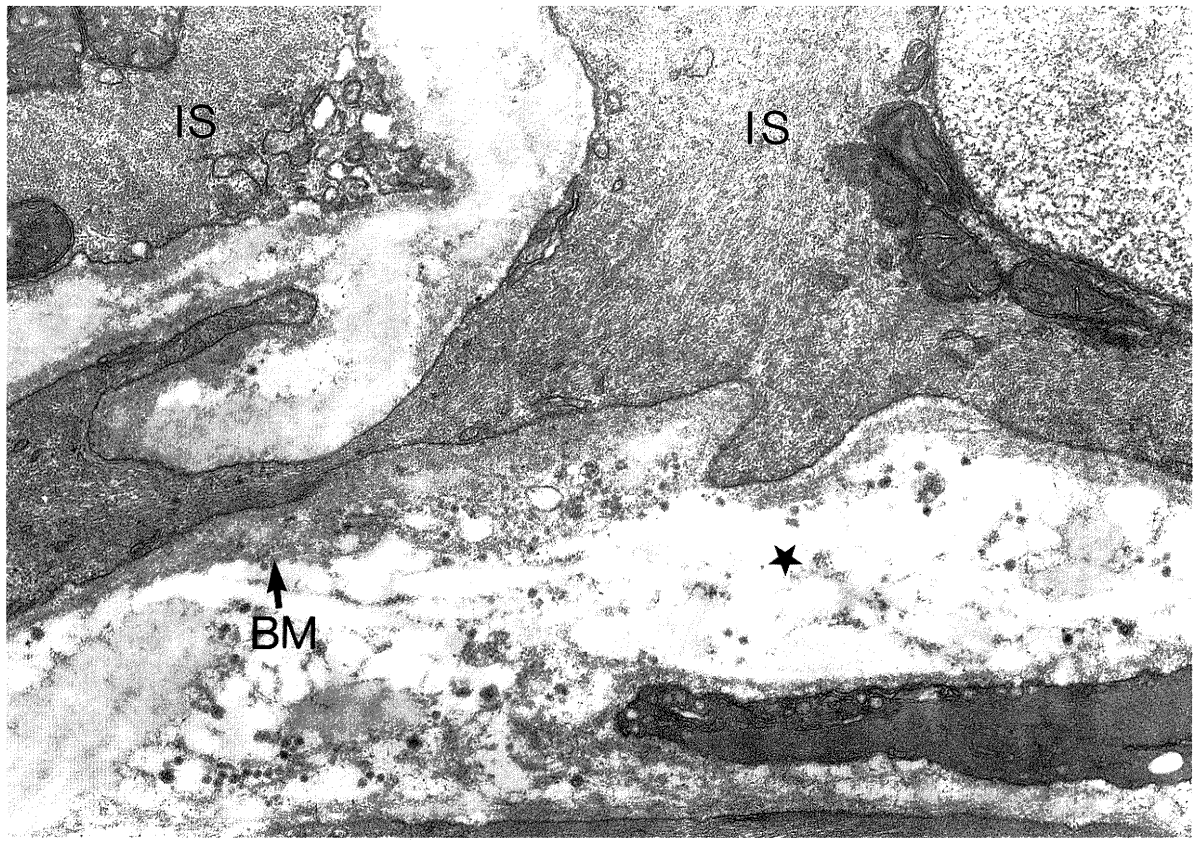

Fig. 11. Electron micrograph of an arterial cushion. Laminated basement membrane-like substances (BM) are found in interstitial space. *IS*: intimal smooth muscle cell. ★: interstitial matrix. ×27,000

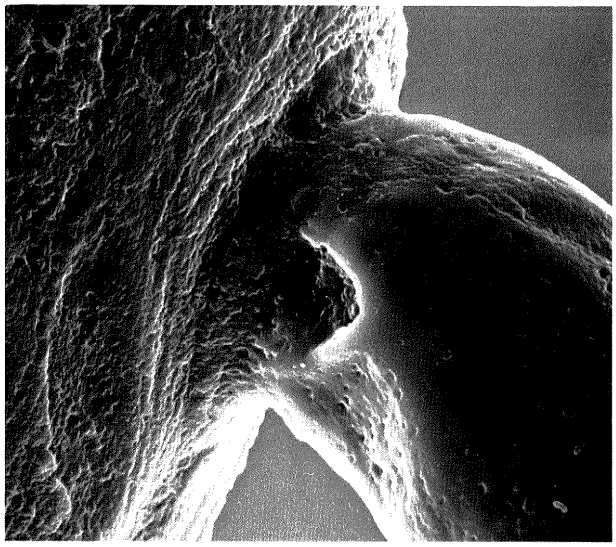

Fig. 12. SEM of methyl metacrylate cast to show arterial cushion.

elongated into the interior of the cushions. Cells of the interior portions of the cushions were modified smooth muscle cells. These cells contained numerous myofibrils and a large number of scattered glycogen granules. No nerve fibers were seen within the cushions. The modified smooth muscle cells were embedded in a loose matrix (probable mucopolysaccharides) which contained strands of basement membrane-like material (Fig. 11).

Under scanning electron microscopy (Fig. 12), the cushions were observed on the wall of the arcuate and interlobular arteries in the cortex, except the subcapsular cortex. They showed elongated indentations surrounding the lumen of their arteries.

DISCUSSION

One of the most important problems of FGS is the vulnerability of glomerular lesions in the juxtamedullary cortex. However, differences among cortical

regions remain unclear in fine vascular structure and hemodynamic mechanisms. Morphometrical analysis of glomerular and vascular structures, including the arterial cushion in intrarenal vessels were therefore attempted.

Values for glomerular diameters have been reported by some investigators, mainly through light microscopic study in which a human kidney was cut at 1-2 μm thick sections. Various diameters of 217 and 160 μm for adults and 161 and 116 μm for children have been obtained.[7,8] These differences were due to considerable variations in glomerular size in the various age groups.[9] These differences may also depend on localization of the glomeruli in different cortical layers. Also doubts exist about values obtained from light microscopic study.

Average values of maximum measurement of glomerular cast by scanning electron micrograph were larger in the juxtamedullary glomeruli. Furthermore, standard deviation of numerical values of efferent arterioles in the juxtamedullary glomeruli showed great variation.

These results are similar to our experimental model of FGS.[10] It was supposed from these results that juxtamedullary glomeruli may show different glomerular hemodynamics and function in individual variations in the juxtamedullary cortex.

Many reports about the experimental model of FGS have described spontaneous renal diseases in aging,[11,12] unilateral nephrectomy,[13] renal ablation,[14] aminonucleoside nephropathy,[15,16] and adriamycin-induced rats.[17]

Functional overload and amino acid toxicity[13] are thought to be responsible for the pathogenesis. More recently it is becoming apparent that glomerular epithelial cell injury is associated with many experimental and clinical glomerular diseases.[18-20] Andrews[21] determined that epithelial cell injury is the primary insult in aminonucleoside of puromycin (PA)-induced nephrosis (AN),[22] and that proteinuria is a secondary response to this injury. Glassor et al.[18] and Velosa et al.[20] demonstrated FGS following long-term administration of PA in rats and concluded that severe visceral epithelial cell injury was the cause of focal sclerosis.

Recently, GBM charge barriers have been implicated as possible causes of proteinuria and many reports concerning anionic sites in the GBM have appeared,[23-25] in addition to reports concerning various anionic sites involved in human glomerulonephritis.[27] However, most of these reports have concerned the GBM and no detailed results regarding anionic sites in the mesangial matrix have emerged in spite of mesangial dysfunction appearing to have an important role in glomerulosclerosis.

In this study, follow-up studies of glomerular sclerosis in AN nephrosis were made to investigate pathogenesis of sclerosis, particularly loss of glomerular polyanion in the GBM, mesangial matrix and arterial cushion.

Intra-arterial cushions have been described in the vessels of many organs and tissues in a variety of species, including man, but particularly well developed in the rat kidney. Accordingly, serial sections of rat kidneys were studied in AN treated rats. Arterial cushions were found in the mid-cortex and juxtamedullary cortex, but not in the subcapsular cortex and without clearly stained colloidal iron staining.

A brief review of the occurrence and distribution of the cushions has been given by Moffat.[28] Arterial cushions at the origins of the juxtamedullary afferent arterioles in kidneys have been described by Taggart & Papp.[29] Fine structure of the cushion has been recently described by Cassellas et al.,[30] Moffat & Creasey[31] and Ono et al.[32] Further quantitative study using PEI is necessary to determine whether loss of anionic sites in arterial cushion occurs on AN nephropathy.

As a result of these observations, the intrarenal arterial cushions are thought to be an important factor in the regulation of glomerular blood flow and disorders of function or autoregulation of intrarenal arteries as anionic loss of the cushion is assumed to lead to glomerular sclerosis. Also, possible etiologic factors in glomerular sclerosis, which have been cited in the literature, are hyperfiltration[33] of single nephrons and anionic loss of the glomerular capillary wall principally due to epithelial cellular injury.[25,34] However, the above data suggest a relation between glomerular sclerosis and the arterial cushion, in which the mesangium shows anionic loss in addition to hyperfiltration and polyanion loss of the GBM.

The above results also demonstrate that the distribution of anionic charge within the mesangial matrix varies in different regions, and that negative charge impairment due to administration of PA was most pronounced in the paramesangial region. This negative charge impairment is believed to promote mesangiolysis and play an important role in glomerular sclerosis.

(This study was supported in part by a Research Grant from the Intractable Disease Division, Public Health Bureau, Ministry of Health and Welfare, Japan.)

REFERENCES

1) Hayslett J P, Krassner LS, Bensch KG, Kashgarian M, Epstein F H: Progression of "lipoid nephrosis" to renal insufficiency. *N Eng J Med* 281: 181-186, 1969.
2) Rich A R: A hitherto undescribed vulnerability of the juxtamedullary glomeruli in lipoid nephrosis. *Bull Johns Hopk Hosp* 100: 173-186, 1957.
3) Habib R: Focal glomerular sclerosis. *Kidney Int* 4: 355-361, 1973.
4) Hyman L R, Burkholder PM: Focal sclerosing glomerulonephropathy with segmented hyalinosis. A clinicopathologic analysis. *Lab Invest* 28: 533-544, 1973.
5) Mizoguchi K, Ishitobi F, Ono H, Iidaka K: The scanning electron microscopical study on plastic model of glomerular vascular system—On autopsy cases—. *Jap J Nephrol* 30: 369-374, 1988. (in Japanese)
6) Schurer J W, Kalicharan D, Hoedemaeker PHJ, Molenaar I: The use of polyethylenimine for demonstration of anionic sites in basement membrane and collagen fibers. *J Histchem Cytophem* 26: 688-689, 1978.
7) Hurley R M, Drummond K N: Glomerular enlargement in primary renal disease. A quantitative study. *Arch Path* 97: 389-391, 1974.
8) Zollinger H U, Mihatsch M J: Renal pathology in biopsy, Springer-Verlag, New York, 1978, p. 28-30.
9) Torhorst J, Mihatsch MJ: Quantitative morphometric analysis of glomerular diseases in kidney biopsies. *Abstr 7th Internat Congr Nephrology Florence,* 1975, p. 315.
10) Mizoguchi K, Ishitobi F, Ono H, Iidaka K: The scanning electron microscopical study of plastic model of glomeruli- Experimental focal glomerular sclerosis in rats-. *Jap J Nephl* 29: 973-980, 1987. (in Japanese)
11) Couser W G, Stilmant M M: Mesangial lesions and focal glomerular sclerosis in the aging rat. *Lab Invest* 33: 491-501, 1975.
12) Elema J D, Arend S A,: Focal and segmental glomerular hyalinosis and sclerosis in the rat. *Lab Invest* 33: 554-561, 1975.
13) Lalich J J, Allen J R: Protein overload nephropathy in rats with unilateral nephrectomy. II. Ultrastructural study. *Arch Pathol* 91: 372-382, 1971.
14) Olson J L, Hostetter T H, Rennke H G, Brenner B M, Venkatachalam M A: Altered glomerular permselectivity and progressive sclerosis following extreme ablation of renal mass. *Kidney Int* 22: 112-126, 1982.
15) Ryan G B, Karnovsky M J: An ultrastructural study of the mechanisms of proteinuria in aminonucleoside nephrosis. *Kidney Int* 8: 219-232, 1975.
16) Saito T, Furuyama T, Kyougoku Y, Yamakage K, Arakawa M, Yoshinaga K: Focal glomerular sclerosis in aminonucleoside nephropathy. *Tohoku J Exp Med* 133: 349-360, 1981.
17) Grond J, Weening J J, Elema J D: Glomerular sclerosis in nephrotic rats. Comparison of the long-term effects of adriamycin and aminonucleoside. *Lab Invest* 51: 277-285, 1984.
18) Grishman E, Churg J: Focal glomerular sclerosis in nephrotic patients: An electron microscopic study of glomerular podocytes. *Kidney Int* 7: 111-122, 1975.
19) Glasser R J, Velosa J A, Micheal AF: Experimental model of focal sclerosis. I. Relationship to protein excretion in aminonucleoside nephrosis. *Lab Invest* 36: 519-526, 1977.
20) Velosa J A, Glasser R J, Nevins T E, Michael A F: Experimental model of focal sclerosis. II Correlation with immunopathologic changes, macromolecular kinetics, and polyanion loss. *Lab Invest* 36: 527-534, 1977.
21) Andrews PM: A scanning and transmission electronmicroscopic comparison of puromycin aminonucleoside induced nephrosis to hyperalbuminemia-induced proteinuria with emphasis on kidney podocyte pedicel loss. *Lab Invest* 36: 183-197, 1977.
22) Schwartz M M, Sharon Z, Pauli B U, Lewis E J: Inhibition of glomerular visceral epithelial cell endocytosis during nephrosis induced by puromycin aminonucleoside. *Lab Invest* 51: 690-697, 1984.
23) Chang R L S, Deen W M, Robertson C R, Brenner B M: Permselectivity of the glomerular capillary wall: III. Restricted transport of polyanions. *Kidney Int* 8: 212-218, 1975.
24) Farquhar M G: The primary glomerular filtration barrier basement membrane or epithelial slits? *Kidney Int* 8: 197-211, 1975.
25) Suzuki Y, Maesawa A, Matsui K, Oite T, Koda Y, Arakawa M: Alteration of glomerular anionic sites by the development of subepithelial deposits inexperimental glomerulonephritis in the rat. *Virchow Arch Cell Pathol* 44: 209-222, 1983.
26) Rennke H G, Patel Y, Venkatachalam MA: Glomerular filtration of proteins: Clearance of anionic, neutral, and cationic horseradish peroxidase in the rat. *Kidney Int* 13: 278-288, 1978.
27) Shirato I, Hanzawa S, Koide H: Alterations of anionic sites on the glomerular basement membrane in human glomerulonephritis. *Jap J Nephl* 29: 1207-1214, 1987 (in Japanese).
28) Moffat D B: Intra-arterial cushions in the arteries of the rat's eye. *Acta Anat* 72: 1-11, 1969.
29) Taggart N E, Rapp J P: The distribution of valves in rat kidney arteries. *Anat Rec* 165: 37-40, 1969.
30) Casellas D, Dupont M, Jover B, Mimran A: Scanning electron microscopic study of arterial cushions in rats: A novel application of the corrosion-replication technique. *Anat Rec* 203: 419-428, 1982.

31) Moffat D B, Creasey M: The fine structure of the intraarterial cushions at the origins of the juxtamedullary afferent arterioles in the rat kidney. *J Anat* 110: 409-419, 1971.
32) Ono H, Mizoguchi K, Ueda Y, Oka K, Iidaka K: Pathomorphological studies on arterial cushion. 1. rat normal kidney. *Jap J Nephrol* 31: 243-251, 1989 (in Japanese).
33) Hostetter Olson J L, Rennke H G, Venkatachalam M A, Brenner BM: Hyperfiltration in remnant nephrons: A potentially adverse response to renal ablation. *Amer J Physiol* 241: F85-F93, 1981.
34) Fishman J A, Karnovsky M J: Effects of the aminonucleoside of puromycin on glomerular epithelial cells in vitro. *Amer J Pathol* 118: 398-407, 1985.